Energy Engineering

Tech Science Press

DOI: 10.32604/EE.2022.015622

ARTICLE

Field Studies on the Removal Characteristics of Particulate Matter and SO_x in Ultra-Low Emission Coal-Fired Power Plant

Xu Zhao, Houzhang Tan, Fuxin Yang* and Shuanghui Deng

Key Laboratory of Thermo-Fluid Science and Engineering, Ministry of Education, Xi'an Jiaotong University, Xi'an, 710049, China

*Corresponding Author: Fuxin Yang. Email: fxyang@xjtu.edu.cn

Received: 31 December 2020 Accepted: 25 March 2021

ABSTRACT

In order to reduce the environmental smog caused by coal combustion, air pollution control devices have been widely used in coal-fired power plants, especially of wet flue gas desulfurization (WFGD) and wet electrostatic precipitator (WESP). In this work, particulate matter with aerodynamic diameter less than 10 μm (PM_{10}) and sulfur oxides (SO_x) have been studied in a coal-fired power plant. The plant is equipped with selective catalytic reduction, electrostatic precipitator, WFGD, WESP. The results show that the PM_{10} removal efficiencies in WFGD and WESP are 54.34% and 50.39%, respectively, and the overall removal efficiency is 77.35%. WFGD and WESP have effects on the particle size distribution. After WFGD, the peak of particles shifts from 1.62 to 0.95 μm, and the mass concentration of fine particles with aerodynamic diameter less than 0.61 μm increases. After WESP, the peak of particle size shifts from 0.95 to 1.61 μm. The differences are due to the agglomeration and growth of small particles. The SO_3 mass concentration increases after SCR, but WFGD has a great influence on SO_x with the efficiency of 96.56%. WESP can remove SO_x, but the efficiency is 20.91%. The final emission factors of SO_2, SO_3, PM_1, $PM_{2.5}$ and PM_{10} are 0.1597, 0.0450, 0.0154, 0.0267 and 0.0215 ($kg \cdot t^{-1}$), respectively. Compared with the research results without ultra-low emission retrofit, the emission factors are reduced by 1~2 orders of magnitude, and the emission control level of air pollutants is greatly improved.

KEYWORDS

Particulate matter; sulfur oxides; wet flue gas desulfurization; wet electrostatic precipitator; coal-fired power plant

1 Introduction

With the rapid urbanization and economic growth, smog is common in large areas of China in recent years. It has adverse effects on people's health and climate change and has attracted more attention [1]. The causes of smog mainly come from air pollutants, such as fine particulate matter (PM, fine PM refers to the particles with aerodynamic diameter less than 2.5 μm), sulfur dioxide (SO_2), and nitrogen oxides (NO_x). The coal-fired flue gas is one of the main sources. According to the Analysis of China Statistical Yearbook, 70% of China's primary energy consumption is coal, of which 75% is used for combustion, while coal-fired power plants (CFPPs) consume about 50%. Moreover, it will take a long time for China's coal-based energy structure to change, so the particulate matter emitted by CFPPs has to receive extensive attention [2,3].

In 2011, the Chinese government issued the "Emission Standard of Air Pollutants for Thermal Power Plants (GB 13223–2011)" [4], which specified the emission concentration of PM, SO_2, $NO_{x,}$ and other air pollutants. The emission limit of PM is 30 $mg \cdot m^{-3}$, and it is 20 $mg \cdot m^{-3}$ in the key areas. In 2014, the "Reformation and Upgrading Action Plan for Coal Energy Conservation and Emission Reduction (2014–2020)" [5] was published by the National Development and Reform Commission, which proposed the ultralow-emission (ULE) standards, requiring the total PM emission concentration to be less than 10 $mg \cdot m^{-3}$. To achieve the ULE, a series of air pollutant emission control devices (APCDs) have been used in CFPPs, including selective catalytic reduction (SCR), electrostatic precipitator (ESP), wet flue gas desulfurization (WFGD), and wet electrostatic precipitator (WESP). In China, most WFGD uses limestone as a desulfurizer, because the limestone raw material is easy to obtain, the cost is low, the operation is stable, the desulfurization efficiency is high, and the by-products with a high utilization rate can be used [6–8]. Moreover, WFGD is retrofitted to improve its desulfurization efficiency in some CFPPs. For example, a double tower wet flue gas desulfurization device is proposed, which is built after the original desulfurization tower. The research showed that the actual operation desulfurization efficiency of the relevant units can reach more than 99.5% [9]. WFGD using a new magnesium-based catalyst has attracted attention because of its small floor area, less pipeline blockage, and less secondary pollution. Nevertheless, the magnesium-based raw materials are distributed unevenly and the reuse of by-products is difficult, so it has not been widely used [10,11].

Furthermore, relevant studies have shown that the installation and use of WFGD will lead to great changes in PM concentration and ion composition in the flue gas. Meij et al. [12] found that after WFGD the PM mass concentration decreased from 100 $mg \cdot m^{-3}$ to 10 $mg \cdot m^{-3}$, and gypsum and limestone appeared in the particles at the outlet. Wang et al. [13] found that in a 300 MW CFPP, the diameter of particles decreased from 3 to 1 μm in WFGD. In addition, the particles changed from regular spherical distribution to irregular blocks easily agglomerated. About 47.5% limestone particles and 7.9% gypsum particles were found in the fine particles at the outlet of WFGD. Lu et al. [14] found that the concentration of Mg^{2+} and Ca^{2+} ions increased significantly after WFGD. Mg and Ca are the main components of WFGD desulfurization slurry. A part of the desulfurization slurry will be converted into fine particles under the interaction of limestone and flue gas, and these particles will be entrained by flue gas. Wu et al. [15] tested four 300 MW coal-fired plants and found that the particle size distribution, mass concentration, and ion composition of particles changed significantly after WFGD. Pan et al. [7] found that after WFGD using limestone, the composition of particles changed and a new particle $CaSO_4$ were formed. Yan et al. [16] found that different desulfurization methods had different effects on the morphology and elemental composition of fine particles. During the desulfurization process, the reaction, evaporation, crystallization, and trapping of high-temperature flue gas and desulfurization slurry may form new fine particles or adsorb on the surface of particles, leading to the changes in the elemental composition and morphology of particles. The effect of WFGD on the concentration of particles depended on the relative strength of slurry spray effect and flue gas entrainment effect, and it also could be affected by flue rate and flue gas temperature. The transition and migration mechanism of flue gas in WFGD is complicated, and further research is needed.

WESP is used as the supplement of flue gas purification equipment [17,18], which has a good removal effect on gypsum droplets, acid mist, toxic heavy metals, fine dust, and other pollutants. Zhang et al. [19] conducted field tests on an ultra-low emission demonstration project of a 1000 MW coal-fired unit and found that the removal efficiency of $PM_{2.5}$ by WESP was 57.3%. Li et al. [20] carried out a particle emission test on six coal-fired power plants with ultra-low emission, and the results showed that WESP had a good removal effect on $PM_{>1}$. However, with the decrease of particle size, the removal efficiency of WESP decreased gradually. The factors affecting the efficiency of WESP to remove particles need to be further studied.

SO_3 is the cause of blue smoke or yellow smoke in CFPPs as well as acid rain. Moreover, it will form secondary particulate sulfate when discharged into the atmosphere, which is also one of the important sources of $PM_{2.5}$ [21,22]. The existing APCDs of CFPPs have a certain effect on SO_3 removal. The test results of typical units by Li et al. [23] showed that the removal efficiency of most WFGD and WESP reached 50%. Wang et al. [24] conducted field tests on the SO_3 concentration of several typical coal-fired units in China. The SO_3 mass concentration in flue gas before WESP was generally lower than 15 $mg \cdot m^{-3}$, and the concentration at the outlet of WESP was less than 5 $mg \cdot m^{-3}$, and the removal efficiency was between 58.0% and 76.5%. Feng et al. [25] found that the SO_3 removal efficiency by WESP in coal-fired units with two-stage WFGD was 23.0%. This might be due to the bipolar desulfurization tower that had a good removal effect on SO_3, and the concentration of SO_3 at the inlet of WESP was very low. This showed that the removal efficiency of WESP is affected by the imported concentration. It is still controversial that the existing flue gas purification devices have a good removal effect on SO_x, and there is no standard emission requirement for SO_3 at this stage. Therefore, it is necessary to study its transformation and migration characteristics in the flue gas to reduce its pollutant emissions.

In order to meet the ULE, many improvements have been made to the existing flue gas purification equipment in CFPPs, but the conversion and migration process of PM and SO_x in the flue gas are complex and affected by many factors. In this work, a coal-fired power plant with ultralow-emission is studied. The original desulfurizing tower is reformed. A spray layer is added between the inlet flue duct of the absorption tower and the first spray layer, and a slurry circulating pump is added. The mode of two-layer flat plate demister is changed into two-layer roof ridge type and one layer pipe type demister, to eliminate the phenomenon of side wall escape of absorption tower and realize absorption tower. In addition, a WESP is installed behind the desulfurization tower to further remove the pollutants in the flue gas. The field test was carried out under full load operation to explore the transformation and migration characteristics of PM and SO_x after the ultralow-emission retrofit.

2 Materials and Methods

2.1 Research Object

The research object is a CFPP in the Beijing-Tianjin-Hebei region. The power plant is equipped with a pulverized-coal boiler and the designed maximum continuous evaporation capacity of the boiler is 2150 $t \cdot h^{-1}$. During the test period, the boiler operated at full load. The combustion coal was bituminous coal. The industrial element analysis results are shown in Table 1.

Table 1: Coal quality analysis

Content	Symbol	Unit	Sample
Total moisture	M_t	%	14
Ash content	A_{ar}	%	11
Carbon	C_{ar}	%	60.16
Hydrogen	H_{ar}	%	3.62
Oxygen	O_{ar}	%	9.94
Nitrogen	N_{ar}	%	0.7
Total sulfur	$S_{t,\ ar}$	%	0.58
Low calorific value	$Q_{net,\ ar}$	$kcal \cdot kg^{-1}$	5445
Dry ash free volatile	V_{daf}	%	36.44

2.2 Test Sampling Point Setting

SCR, ESP, WFGD, and WESP are installed in the test unit after ultralow-emission transformation. As shown in Fig. 1, five sampling sites were selected in the test, which was located at the inlet of SCR, the outlet of SCR, the outlet of ESP, the outlet of WFGD, and the outlet of WESP. The measurement of SO_2 and SO_3 were measured at four samplings (Points A, B, D, and E), while the measurement of particulate matter was sampled at sites after ESP.

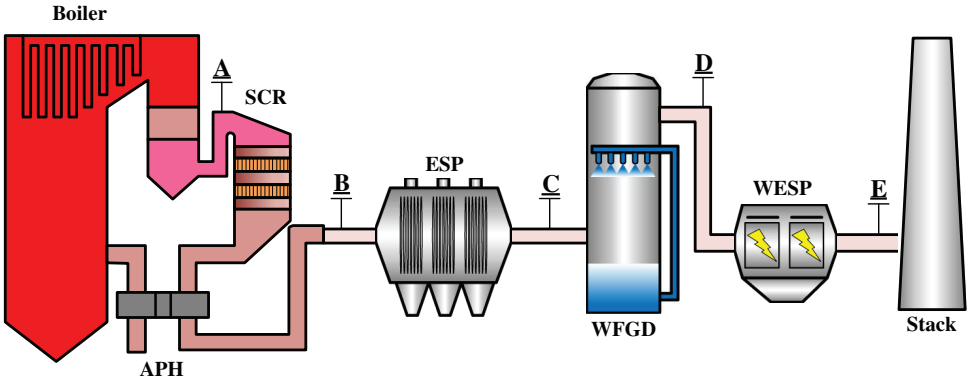

Figure 1: Schematic diagram of sampling points

2.3 Sampling and Analysis Methods

According to "The Determination of Particulates and Sampling Methods of Gaseous Pollutants Emitted from Exhaust Gas of Stationary Source" (GB/T 16157-1996) and "Determination of Particulate Matter Emissions from Stationary Sources" (EPA method 5, 17), the isokinetic sampling method was used to determine the mass concentration of PM in the flue gas. According to the actual situation of the test sample, the sampling time of each sampling point was set. The angle between the central axis of the sampling nozzle and the direction of flue gas flow should be less than 5°.

The sampling device is shown in Fig. 2. The sampling device was mainly composed of a sampling gun, cyclone separator, Dekati low-pressure impact instrument (DLPI), vacuum pump, etc. According to the sampling flow rate (extraction flow rate is 10 $L \cdot min^{-1}$) and flue gas flow rate, the appropriate sampling nozzle was selected to realize isokinetic sampling. In the sampling process, the sampling gun was used to extract the flue gas from the flue gas. Firstly, the cyclone separator was used to remove and collect the particles with aerodynamic diameter greater than 10 μm in the flue gas, and then went into DLPI. The particles in the DLPI were divided into 13 grades due to their different aerodynamic diameters, and then they were collected separately. DLPI used the principle of inertial collision to classify particles. The collecting base of particles in the device was made of aluminum foil coated with Apiezon-H silicone grease. Before and after measurement, the Sartorius BP211D microanalysis balance was used to weigh the aluminum foil. The mass difference obtained was the mass distribution information of particles in different stages. To avoid the influence of moisture and acid gas condensation on the measurement results, the heating sleeve was used to heat the sampling gun, cyclone separator, DLPI, and connecting pipe during the sampling process, and the temperature should not be lower than 403.15 K.

As shown in Fig. 3, the SO_3 sampling test is based on "Performance Test Method for Coal-fired Flue Gas Desulfurization Equipment (GB/T 21508-2008)", which was mainly composed of sampling gun, quartz filter, serpentine glass collecting pipe, droplet separator, and vacuum pump. A quartz filter was used to filter PM in the flue gas. During measurement, the quartz filter and sampling gun should be heated to

473.15 K to prevent condensation of water vapor and acid gas. At the same time, the absorption bottle needed to be placed in a water bath, the bath temperature was not higher than 303.15 K. The sample flow was kept at a constant rate of about 10.0 L/min for 30–60 min After sampling, the glass tube and quartz filter needed to be washed with deionized water, and then the washing liquid would be added and converted to the concentration of SO_3. The concentration was determined by Barium-Thorin titration. In the titration process, the resin was used to remove NH_4^+ and other impurity ions. Before the use, the resin was treated using sodium hydroxide and hydrochloric acid solution. Moreover, each sample was titrated several times and the average value was adopted to eliminate the biases.

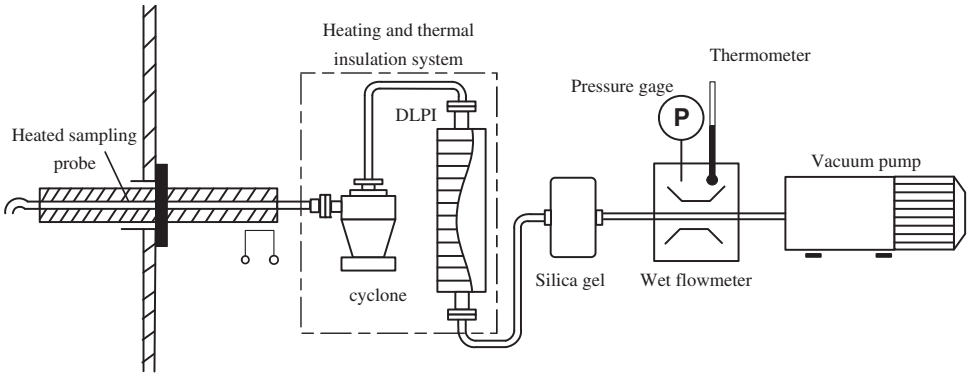

Figure 2: Schematic diagram of particulate matter sampling system

2.4 Composition Analysis of the Flue Gas

According to the requirements of "The Determination of Particulates and Sampling Methods of Gaseous Pollutants Emitted from Exhaust Gas of Stationary Source" (GB/T 16157-1996), a calibrated flue gas analyzer was used to obtain the composition analysis of the flue gas. The concentration of each grid point was converted to the same oxygen content for arithmetic average, and the result was the flue gas composition concentration of the section, and the CEMS of the unit was checked.

2.5 Calculation of Emission Factors

Taking fuel consumption as the basic unit, establish SO_x and PM emission factors, which represent the emission of 1 t coal consumed per unit, respectively [26]. The formula is as follows:

$$EF_e = C \times \frac{Q_{gas}}{M_{fuel} \times 10^6}$$

where EF_e is the emission factor ($kg \cdot t^{-1}$), C is the pollutant concentration ($mg \cdot m^{-3}$), Q_{gas} is the flue gas emission ($m^3 \cdot h^{-1}$), M_{fuel} is the coal consumption ($t \cdot h^{-1}$). The emission factors of PM_1, $PM_{2.5,}$ and PM_{10} need to be converted according to the emission factors, and the formula is as follows:

$$EF_{PM} = EF_e \times Y$$

where EF_{PM} is the emission factor ($kg \cdot t^{-1}$), Y is the conversion coefficient. The conversion coefficient of PM_1, $PM_{2.5,}$ and PM_{10} are 0.9896, 0.9354, and 0.6584, respectively.

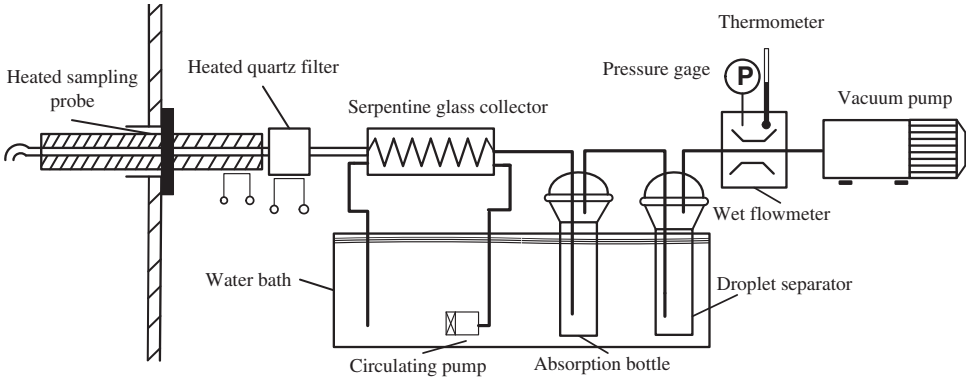

Figure 3: Schematic diagram of the SO_3 sampling system

3 Result and Discussion

3.1 Emission Characteristics of Particulate Matter at the Inlet and Outlet of WFGD and WESP

The PM mass concentration at the inlet and outlet of WFGD and WESP of coal-fired units was tested by DLPI divided into 13 grades. Table 2 shows the PM mass concentration and cumulative percentage of each stage of DLPI. The mass concentration of PM_{10} at the inlet of WFGD is 15.345 $mg \cdot Nm^{-3}$. At the outlet of WFGD, the mass concentration of PM_{10} is 7.007 $mg \cdot Nm^{-3}$, and the removal efficiency is 54.34%. At the outlet of WESP, the mass concentration of PM_{10} decreases to 3.476 $mg \cdot Nm^{-3}$, and the total removal efficiency is 50.39%. After WFGD and WESP, the efficiency is 77.35%, but the proportion of $PM_{2.5}$ increases from 73.7% to 88.7%.

Table 2: PM mass concentrations at inlet and outlet of WFGD and WESP

Particle size D_{50} (μm)	WFGD inlet		WFGD outlet		WESP outlet	
	Cumulative ($mg \cdot Nm^{-3}$)	Cumulative (%)	Cumulative ($mg \cdot Nm^{-3}$)	Cumulative (%)	Cumulative ($mg \cdot Nm^{-3}$)	Cumulative (%)
0.023	0.139 ± 0.035	1.3	0.239 ± 0.035	5.3	0.064 ± 0.001	2.4
0.048	0.412 ± 0.067	3.1	0.577 ± 0.053	10.5	0.140 ± 0.003	4.8
0.083	0.776 ± 0.111	5.6	0.961 ± 0.042	16.5	0.241 ± 0.002	7.9
0.144	1.129 ± 0.102	8.1	1.426 ± 0.043	24.1	0.339 ± 0.004	11.1
0.254	1.631 ± 0.064	10.6	1.957 ± 0.050	30.1	0.478 ± 0.002	14.3
0.378	2.145 ± 0.218	13.8	2.505 ± 0.025	37.6	0.679 ± 0.005	19.8
0.615	2.936 ± 0.542	18.1	3.111 ± 0.010	45.1	1.093 ± 0.067	30.2
0.957	4.834 ± 1.298	30.6	4.386 ± 0.506	63.9	1.657 ± 0.114	46.8
1.619	8.665 ± 1.757	50.0	5.584 ± 0.067	77.4	2.463 ± 0.279	65.1
2.426	12.352 ± 1.486	73.7	6.368 ± 0.052	88.7	3.041 ± 0.098	81.7
4.060	13.708 ± 0.424	82.5	6.786 ± 0.068	94.7	3.261 ± 0.002	88.1
6.800	14.720 ± 0.204	87.5	6.923 ± 0.032	96.2	3.369 ± 0.006	90.5
10.000	15.345 ± 0.108	100.0	7.007 ± 0.010	100.0	3.476 ± 0.001	100.0

Fig. 4 shows the mass concentration distribution and removal efficiency of particles with different particle sizes in the desulfurization process. At the inlet and outlet of WFGD, the concentration of PM presents a single peak distribution. The peak appears at the aerodynamic diameter of 1.62 μm at the inlet of WFGD, mainly concentrated in 0.957~6.80 μm. At the outlet of WFGD, the peak of PM appears at the aerodynamic diameter of 0.95 μm and the main particle concentration is $PM_{2.5}$. But the proportion of PM_1 increases to 63.9%. The peak of mass concentration distribution shifts to smaller particles after WFGD. The removal efficiency of particles with aerodynamic diameter less than 0.61 μm by WFGD is negative, indicating that WFGD has a negative effect on the removal of these particles and will increase the mass concentration. When the particle size is greater than 0.61 μm, the removal efficiency increases with the increase of particle size.

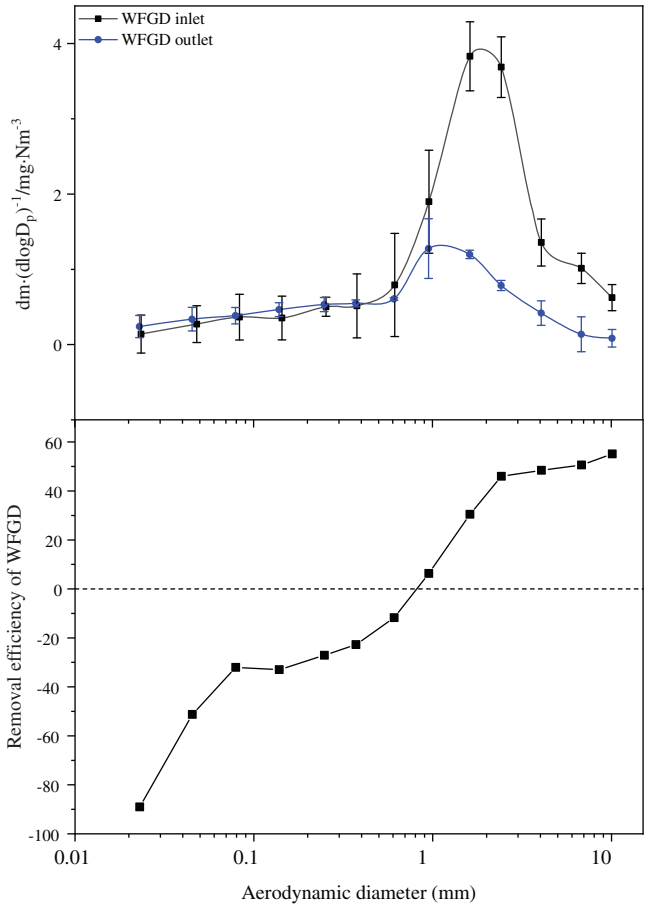

Figure 4: Part size distributions and removal efficiency in WFGD

By comparing the mass concentration distribution of different particle sizes in WFGD inlet and outlet, it can be concluded that WFGD has a good removal effect on the larger particles, but it has no removal effect for the particle with the size less than 0.61 μm. Instead, it increases the mass concentration of fine particles in the flue gas, causing the peak of mass concentration distribution at the WFGD outlet to shift to the smaller particles reason.

After entering the desulfurization tower, the flue gas and desulfurization slurry exchange heat rapidly, then the temperature of the flue gas decreases to below the acid dew point, and most of the sulfuric acid vapor form submicron sulfuric acid droplets. The sulfuric acid droplets with particle size greater than 10

μm will be absorbed and trapped by the slurry of desulfurization tower, and the sulfuric acid droplets with particle size of 0.5~3.0 μm will form aerosol, which is difficult to remove [24]. In the related research [13,15], it was also found that the mass concentration of fine particles increases after WFGD. The effect of WFGD on particles can be divided into two parts, one is the washing effect of spray slurry for particles, and the other is the carrying effect of high temperature flue gas. The large size particles are easy to be absorbed and removed by the spray slurry, which significantly reduces the mass concentration of particles. However, the fine particles are not easy to be captured and removed by the spray slurry, and a large part of them will still flow out of the desulfurization tower with the flue gas. At the same time, the reaction, evaporation, and other effects will occur between the high temperature flue gas and desulfurization slurry, which produce desulfurizer crystal and other fine particles. The particles originally carried in the flue gas will also react with the desulfurization slurry to generate new particle crystals [7], which will be carried out of the desulfurization tower with the flue gas. This will increase the mass concentration of fine PM in the flue gas after WFGD.

Fig. 5 shows the mass concentration distribution and removal efficiency of particles with different particle sizes at the inlet and outlet of WESP. It is shown that the mass concentration of PM still presents a single peak distribution. The peak of PM occurs at 0.95 μm at the WESP inlet. The main concentration of PM is $PM_{2.5}$, and the proportion of PM_1 reaches 63.9%. At the outlet of WESP, the peak of PM appears at 1.62 μm, and the main contributor is the fine particles with particle size of 0.61~2.42 μm, accounting for 51.5%. The peak of WESP outlet mass concentration distribution shifts to larger particles. The results show that the removal efficiency of WESP for particles with particle size of 0.02~0.95 μm is 62.2~76.2%, and it is 50.4~55.9% for 0.95~10.09 μm. WESP has good removal effects for all sizes of particles, but when compared with large particle size, WESP has a better removal effect on PM_1 particles. This is one of the reasons that the peak of WESP outlet mass concentration distribution shifts to larger particles. Another possible reason is that under the action of the WESP electric field and other fields, fine particles are agglomerated to form larger particles.

WESP mainly depends on electrostatic force, fluid drag force, thermophoresis force, and liquid bridge force to remove particles from flue gas. When the droplets are injected into the electric field, the distribution area of high potential becomes wider, which is conducive to the collection of particles [27]. The particles with the size of 0.1~1.0 μm belong to the difficult charging area [28], so the removal efficiency is lower than that of other particle sizes. Zhao et al. [29] found that the removal efficiencies of WESP for PM_{10}, $PM_{2.5,}$ and PM_1 were 79.6%, 77.0%, and 75.9%, respectively. The larger the particle size, the higher the removal efficiency, and the proportion of PM_1 increased after WESP. In the study of Wu et al. [15], the average removal efficiencies of WESP for $PM_{2.5}$, $PM_{2.5–10,}$ and $PM_{>10}$ were 59%, 64%, and 45%, respectively. Although the removal efficiency of $PM_{2.5–10}$ was higher than that of $PM_{2.5,}$ the removal efficiency of $PM_{>10}$ with a larger particle size decreased. The removal of particulates in flue gas by WESP is affected by many aspects. In addition to the influence of particle size, the influence of voltage, current, flue gas flow, and humidity during WESP operation should be considered. In the test, WESP uses a three-phase power supply, and the DC voltage during operation is 80000 V. The WESP has a removal efficiency of 67.9% for mist droplets, so a part of the mist droplets will be carried out of the WESP by the flue gas. This will affect the composition of the particulate matter in the flue gas.

3.2 Removal Characteristics of Sulfur Oxides by WFGD and WESP

Table 3 and Fig. 6 show the removal efficiency of SO_x by APCDs. At the inlet of SCR, the mass concentrations of SO_3 and SO_2 are 5.15 $mg \cdot Nm^{-3}$ and 797 $mg \cdot Nm^{-3}$, respectively. After SCR, the mass concentration of SO_3 increases, while the mass concentration of SO_2 decreases. At the outlet of SCR, the mass concentration of SO_3 is 19.28 $mg \cdot Nm^{-3}$, and the mass concentration of SO_2 is 782 $mg \cdot Nm^{-3}$. The removal efficiency is −274% and 1.88% for SO_3 and SO_2, respectively. SCR is designed to remove NO_x

in flue gas, which has little effect on the removal of SO_x. The principle of SCR for NO_x removal is that under the action of catalyst, the reducing agent selectively reacts with NO_x in the flue gas to generate environmentally friendly N_2 and H_2O, but at the same time, the catalyst can also oxidize some of SO_2 in the flue gas to SO_3. SO_3 will react with unreacted ammonia in SCR to produce NH_4HSO_4. NH_4HSO_4 is viscous, which will harm the catalytic bed and air preheater, and affect the morphology and elemental composition of particulates in flue gas [30,31]. In general, the conversion rate of SO_2/SO_3 in SCR of CFPPs is between 0.25~1.25% [32], and some studies have shown that the conversion rate of SO_2/SO_3 is 0.5~2.0% through SCR [33]. In this test, the conversion rate is 0.91%, which meets the design and environmental requirements.

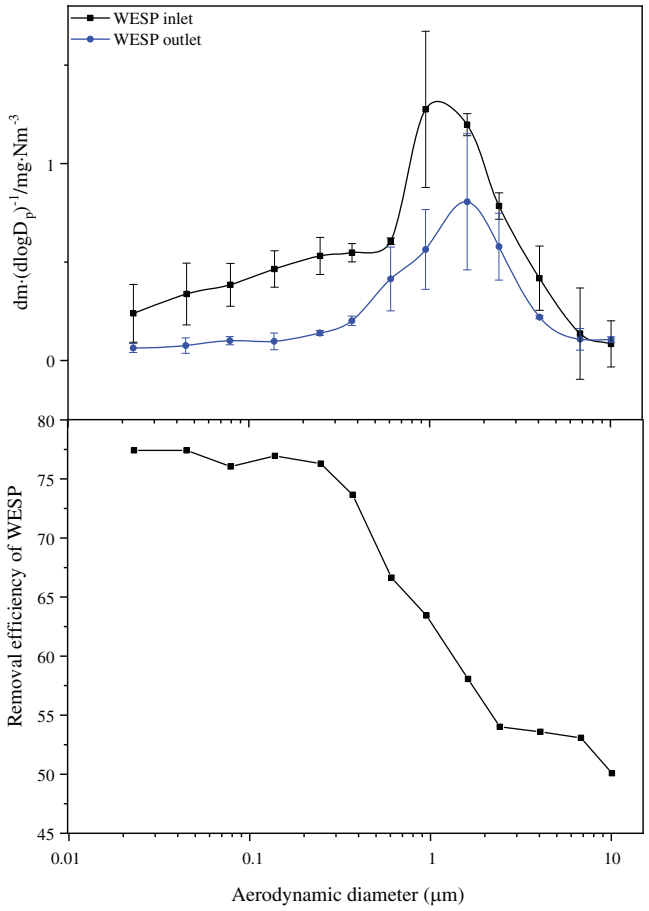

Figure 5: Part size distributions and removal efficiency in WESP

After WFGD, the mass concentration of SO_2 and SO_3 decreases. WFGD has a great influence on SO_x with efficiencies of 96.56%. The mass concentration of SO_2 decreases to 20 $mg \cdot Nm^{-3}$, and the removal efficiency is 97.44%. Meanwhile, the mass concentration of SO_3 decreases to 7.55 $mg \cdot Nm^{-3}$, and the removal efficiency is 60.84%. After entering WFGD, The flue gas temperature will rapidly drop below the acid dew point, SO_3 will combine with water in the flue gas and form a sulfuric acid aerosol. The slurry of absorption tower is sprayed from top to bottom and reversely intersects with flue gas, which neutralizes acid SO_2 and removes part of the sulfuric acid mist. Due to the high velocity of flue gas and the short contact time between spray slurry and flue gas, the speed of sulfuric acid fog formation is

greater than that of slurry absorbing sulfuric acid mist. The larger particle size of sulfuric acid fog aerosol is intercepted due to inertial collision and is removed by reaction with slurry [23,34]. However, the submicron sulfuric acid aerosol with a smaller particle size is not easy to be intercepted and trapped, so the removal efficiency is not high. Relevant researchers [35] have tested the removal efficiency of several limestone gypsum desulfurization units, and the removal rate was 42.1%~77.8%. In this test, the removal efficiency is 60.84%, which is in accordance with the previous studies.

Table 3: Concentration distribution and removal efficiency of SO_x in APCDs

	Concentration/mg · Nm^{-3}				Removal efficiency/%		
SO_x	SCR inlet	SCR outlet	WFGD outlet	WESP outlet	SCR	WFGD	WESP
SO_2	797 ± 24.65	782 ± 8.36	20 ± 2.17	17 ± 1.45	1.88	97.44	15
SO_3	5.15 ± 0.38	19.28 ± 0.81	7.55 ± 0.16	4.79 ± 0.06	−274.37	60.84	36.56

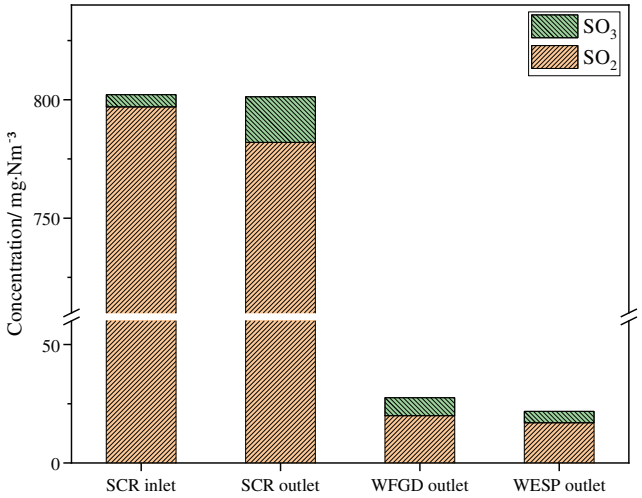

Figure 6: Concentration distribution of SO_x in APCDs

After WESP, the flue gas will be discharged into the atmosphere from the chimney. The mass concentration of SO_x measured at the outlet of WESP is the final mass concentration of CFPP. At the outlet of WESP, the mass concentrations of SO_2 and SO_3 are 17 mg · Nm^{-3} and 4.79 mg · Nm^{-3} respectively, and the removal efficiencies are 15% and 36.56%, respectively. It can be seen that WESP has a certain removal effect on SO_x, but the removal efficiency is only 20.91%. WESP has the advantages of multiple pollutants coordinated control, especially for the removal of fine particles. After entering WESP, SO_3 in flue gas mainly exists in the form of a submicron sulfuric acid aerosol, which belongs to the category of fine particles [36]. According to the research on WESP in many CFPPs [23,35,37], the removal efficiency of SO_3 is generally 52.2~90.4%. In contrast, the SO_3 removal efficiency in this study is relatively low. The reason may be that the SO_x concentration at the inlet of WESP is very low, and only a small part of submicron sulfuric acid aerosol particles are charged for removal, which results in the low removal efficiency of WESP.

The removal of SO_2 in WESP is based on the gas-liquid diffusion, coupled with the effect of electric field force and active groups [38]. Yang et al. [39] have proved that corona discharge can enhance the

absorption of SO_2 by droplets, especially for low concentration SO_2. The removal efficiency reaches 79.8%. However, the laboratory research and the actual test in the engineering site are different. In practical application, the situation is often more complex and changeable. Li et al. [34] found that the removal efficiency of SO_2 by WESP is 19.6~24.8%, which is close to the test results.

In the study, the overall removal efficiency of SO_2 by air pollutant emission control device is 97.87%, and the removal efficiency of SO_3 is 6.99%. The mass concentration at the outlet of the chimney meets the requirements of the emission standard.

3.3 Emission Factors of Particulate Matter and SO_x

During the test, the flue gas rate was 2319935 $m^3 \cdot h^{-1}$, and the standard coal consumption was 247 $t \cdot h^{-1}$. According to the above formula, the final emission factors of pollutants from coal-fired units are calculated, and the emission factors of SO_2 and SO_3 are 0.1597 and 0.0450 ($kg \cdot t^{-1}$), and the emission factors of PM_1, $PM_{2.5,}$ and PM_{10} are 0.0154, 0.0267 and 0.0215 ($kg \cdot t^{-1}$), respectively. Wang et al. [24] studied the emission characteristics of PM from CFPPs without ultralow-emission retrofit, and the results showed that the emission factors of $PM_{2.5}$, $PM_{10,}$ and total dust were 0.747~0.1855, 0.1424~0.3545, and 0.1561~0.3852 ($kg \cdot t^{-1}$), respectively. Liu et al. [26] found that the emission factors from coal-fired units with ultra-low emissions in Haikou of SO_2, PM_1, $PM_{2.5,}$ and PM_{10} were 0.1131, 0.0065, 0.0092, and 0.0098 ($kg \cdot t^{-1}$), respectively. Compared with the research results, the emission factors were reduced by 1~2 orders of magnitude. Li et al. [20] explored the emission characteristics of PM from coal-fired units, and the emission factors of PM_1, $PM_{2.5}$ and PM_{10} were 0.0062~0.019, 0.0059~0.016 and 0.0059~0.017 ($kg \cdot t^{-1}$), respectively. Compared with the results of the existing research on ultra-low emission coal-fired units, the emission factor studied in this work is slightly higher, and compared with the coal-fired units without ultra-low emission retrofit, the emission control level of air pollutants has been greatly improved.

4 Conclusion

This work studies the effects of WFGD and WFGD on PM and SO_x in flue gas after ultra-low emission conversion, and the following conclusions are as follows:

(1) WFGD and WESP have good removal effects on PM, with a removal efficiency of 54.34% and 50.39%, respectively. The overall removal efficiency is 77.35%. After WFGD, the peak of PM shifts from 1.62 to 0.95 μm, and WFGD has a negative effect on fine particles with a diameter less than 0.61 μm. The main reasons are the entrainment of small droplets with the flue gas, which are difficult to remove and easy to escape from the desulfurization tower.

(2) After WESP, the particle size peak shifts from 0.95 to 1.61 μm with a larger particle size. This should be due to the agglomeration and growth of small particles under the action of WESP. However, the cumulative removal efficiency of WESP decreases with the increase of particle size, which is different from previous studies. Therefore, it is necessary to further study the influencing factors of WESP removal.

(3) SCR increases the mass concentration of SO_3 by 274%, which is due to the oxidation of SO_2 to SO_3 by SCR catalyst. WFGD has a good effect on SO_x removal, and the removal efficiencies of SO_2 and SO_3 reach 97.44% and 60.84%, respectively. WESP also has a certain effect on SO_x removal, but the efficiency is not high. The reason may be that the concentration of SO_3 at the entrance of WESP is low, and the SO_3 aerosol is difficult to charge.

(4) The emission factors of SO_2, SO_3, PM_1, $PM_{2.5}$ and PM_{10} are 0.1597, 0.0450, 0.0154, 0.0267 and 0.0215 ($kg \cdot t^{-1}$). Compared with the research results without ultra-low retrofit, the emission factors have been reduced by 1~2 orders of magnitude, and the air pollutant emission control level is greatly improved.

Funding Statement: The work was supported by the National Key Research and Development Plan of China (No. 2016YFB0600605).

Conflicts of Interest: The authors declare that they have no conflicts of interest to report regarding the present study.

References

1. Wang, H. J., Chen, H. P. (2016). Understanding the recent trend of haze pollution in eastern China: Roles of climate change. *Atmospheric Chemistry and Physics, 2016,* 1–18. DOI 10.5194/acp-16-4205-2016.
2. Ding, M., Yu, J. Q., Zhen, C., Chen, Y. Z. (2014). Analysis of $PM_{2.5}$ ambient particulars emission source of nanjing. *Environmental Science and Technology, 27(4),* 23–26. DOI 10.3969/j.issn.1674-4829.2014.04.006.
3. Sui, J. C., Du, Y. G., Xu, M. H., Li, Y. (2008). Status quo of the study on the development of coal combustion in China and its development trend. *Journal of Engineering for Thermal Energy and Power, 23(2),* 111–116 + 212. DOI CNKI:SUN:RNWS.0.2008-02-002.
4. Emission Standard of Air Pollutants for Thermal Power Plants (GB 13223-2011). Ministry of environmental protection of the people's republic of China, general administration of quality supervision, inspection and quarantine.
5. Reformation and Upgrading Action Plan for Coal Energy Conservation and Emission Reduction (2014). National Development and Reform commission, Ministry of Environmental Protection of the People's Republic of China, National Energy Administration.
6. Córdoba, P. (2015). Status of flue gas desulphurization (FGD) systems from coal-fired power plants: Overview of the physic-chemical control processes of wet limestone FGDs. *Fuel, 144,* 274–286. DOI 10.1016/j.fuel.2014.12.065.
7. Pan, D. P., Wu, H., Yang, L. J. (2016). Fine particle transformation during the limestone gypsum desulfurization process. *Energy Fuels, 30(11),* 9737–9744. DOI 10.1021/acs.energyfuels.6b01133.
8. Yao, S., Cheng, S. Y., Li, J. B., Zhang, H. Y. et al. (2019). Effect of wet flue gas desulfurization (WFGD) on fine particle ($PM_{2.5}$) emission from coal-fired boilers. *Journal of Environmental Sciences, 77,* 32–42. DOI 10.1016/j.jes.2018.05.005.
9. Wei, H. G., Xu, M. H., Chai, L., Zhu, Y. (2016). Current operation state analysis and optimization method exploration on double-tower double-cycle wet-FGD systems. *Electric Power, 49(10),* 132–135. DOI 10.11930/j.issn.1004-9649.2016.10.132.04.
10. Lin, H. J., Lin, Y. Q., Wang, D. H., Pang, Y. W., Zhang, F. B. et al. (2018). Ammonium removal from digested effluent of swine wastewater by using solid residue from magnesium-hydroxide flue gas desulfurization process. *Journal of Industrial and Engineering Chemistry, 58,* 148–154. DOI 10.1016/j.jiec.2017.09.019.
11. Ma, Y. P., Yuan, D. L., Mu, B. L., Gao, L., Zhang, X. J. et al. (2018). Synthesis, properties and application of double salt $(NH_4)_2Mg(SO_4)_2 \cdot 6H_2O$ in wet magnesium-ammonia FGD process. *Fuel, 219,* 12–16. DOI 10.1016/j.fuel.2018.01.055.
12. Meij, R., Te Winkel, B. (2003). The emissions and environmental impact of PM_{10} and trace elements from a modern coal-fired power plant equipped with ESP and wet FGD. *Fuel Processing Technology, 85(6–7),* 641–656. DOI 10.1016/j.fuproc.2003.11.012.
13. Wang, H., Song, Q., Yao, Q., Chen, C. H. (2008). Experimental study on removal effect of wet flue gas desulfurization system on fine particles from a coal-fired power plant. *Proceeding of the CSEE, 28(5),* 1–7. DOI 10.3321/j.issn:0258-8013.2008.05.001.
14. Lu, P., Wu, J., Pan, W. P. (2010). Particulate matter emissions from a coal-fired power plant. In: *Bioinformatics and Biomedical Engineering*, pp. 1–4. *4th IEEE International Conference,* Chengdu.
15. Wu, B. B., Tian, H. Z., Hao, Y., Liu, S. H., Liu, X. Y. et al. (2018). Effects of Wet flue Gas desulfurization and Wet electrostatic precipitators on emission characteristics of particulate matter and its ionic compositions from four

300 MW level ultralow coal-fired power plants. *Environmental Science & Technology, 52(23),* 14015–14026. DOI 10.1021/acs.est.8b03656.

16. Yan, J. P., Yang, L. J., Bao, J. J. (2011). Impact property on fine particles from coal combustion in wet flue gas desulfurization process. *Journal of Southeast University (Natural Science Edition), 41(2),* 387–392. DOI 10.3969/j.issn.1001-0505.2011.02.033.
17. Liu, H. H., Tao, Q. G. (2012). Exploration application of wet electric dust catcher to engineering. *Electric Power Survey & Design, 2012(3),* 43–47. DOI 10.3969/j.issn.1671-9913.2012.03.010.
18. Mo, H., Zhu, F. H., Wang, S., Yi, Y. P. (2013). Application of WESP in coal-fired power plants and its effect on emission reduction of $PM_{2.5}$. *Electric Power, 46(11),* 62–65. DOI 10.3969/j.issn.1004-9649.2013.11.013.
19. Zhang, J., Zheng, C. H., Zhang, Y. X., Wu, G. C., Zhu, S. Q. et al. (2016). Experimental investigation of ultra-low pollutants emission characteristics from a 1000 MW coal-fired power plant. *Proceedings of the CSEE, 36(5),* 1310–1314. DOI 10.13334/j.0258-8013.pcsee.2016.05.016.
20. Li, X. L., Zhou, D. B., Duan, J. X., Zhang, W. J., Li, J. Z. et al. (2018). Characteristics of particle emission from coal-fired power plants under the ultra low emission standard. *Environmental Monitoring in China, 34(3),* 45–50. DOI 10.19316/j.issn.1002-6002.2018.03.07.
21. Liu, H. X., Yao, Y. P., Li, J. G., Shen, Z. A., Zhu, S. P. et al. (2015). Study on SO_3 generation, control and testing technology for coal-fired power plants. *Electric Power, 48(9),* 152–156. DOI CNKI:SUN:ZGDL.0.2015-09-033.
22. Wang, H. L., Xue, J. M., Xu, Y. Y., Li, B., Chen, M. J. (2014). Formation and control of SO_3 from coal-fired power plants. *Electric Power Technology and Environmental Protection, 30(5),* 17–20. DOI 10.3969/j.issn.1674-8069.2014.05.006.
23. Li, X. L., Li, J. Z., Duan, J. X., Yi, Y. P., Zhang, W. J. (2019). SO_3 cooperative control and emission situation in the flue gas of coal-fired power plant. *Electric Power, 52(10),* 155–161. DOI 10.11930/j.issn.1004-9649.201808069.
24. Wang, D. B., Lei, M., Yu, F. S., Niu, Y. J., He, Y. D. et al. (2018). SO_3 migration and emission characteristics of coal-fired power units. *Thermal Power Generation, 47(11),* 96–101. DOI 10.19666/j.rlfd.201803074.
25. Feng, P., Li, Z. H., Liu, H. X., Tan, H. Z., Zhang, S. C. et al. (2020). Migration and removal characteristics of SO_3 in ultra-low emission coalfired power plant. *Chemical Industry and Engineering Progress, 39(11),* 4660–4667. DOI 10.16085/j.issn.1000-6613.2020-0186.
26. Liu, Y. M., Yan, J., Xu, W. S., Yan, X., Sun, X. S. et al. (2020). Emission characteristics of conventional air pollutants in coal-fired power plants after ultra-low emission transformation. *Acta Scientiae Cricumstantiae, 40(6),* 1967–1975. DOI 10.13671/j.hjkxxb.2020.0010.
27. Liu, H. X., Yao, Y. P., Li, J. G., Chen, Z. M., Fang, X. W. (2017). Research of PM removal mechanism and emission characteristics for WESP in a coal-fired power plant. *Electric Power, 50(12),* 178–184. DOI 10.11930/j.issn.1004-9649.201706180.
28. Luo, Z. Y., Jiang, J. P., Zhao, L., Chen, H., Fang, M. X. et al. (2014). Research on the charging of fine particulate in different electric fields. *Proceedings of the CSEE, 34(23),* 3959–3969. DOI 10.13334/j.0258-8013.pcsee.2014.23.017.
29. Zhao, L., Zhou, H. G. (2016). Particle removal efficiency analysis of WESP in an ultra Low emission coal-fired power plant. *Proceedings of the CSEE, 36(2),* 468–473. DOI 10.13334/j.0258-8013.pcsee.2016.02.018.
30. Wu, B. G., Wang, S. G., Sheng, Y. X. (2006). Flue gas denitrification technologies and analysis of their chemical reactions. *Thermal Power Generation, 2006(11),* 59–60+64+77. DOI 10.3969/j.issn.1002-3364.2006.11.020.
31. Ma, S. C., Jin, X., Sun, Y. X., Cui, J. W. (2010). The formation mechanism of ammonium bisulfate in scr flue gas denitrification process and control thereof. *Thermal Power Generation, 39(8),* 12–17. DOI 10.3969/j.issn.1002-3364.2010.08.012.
32. Srivastava R, K., Miller C, A., Erickson, C., Jambhekar, R. (2004). Emissions of sulfur trioxide from coal-fired power plants. *Journal of the Air & Waste Management Association, 54(6),* 750–762. DOI 10.1080/10473289.2004.10470943.
33. Cao, Y., Zhou, H. C., Jiang, W., Chen, C. W., Pan, W. P. (2010). Studies of the fate of sulfur trioxide in coal-fired utility boilers based on modified selected condensation methods. *Environmental Science & Technology, 44(9),* 3429–3434. DOI 10.1021/es903661b.

34. Li, Q. Y., Hu, D. Q., Zhang, J., Gao, X. (2017). Synergistic removal of WFGD and WESP on gas pollutants with ultra low emission. *Journal of Engineering for Thermal Energy and Power, 32(8),* 138–143 + 154. DOI 10.16146/j.cnki.rndlgc.2017.08.022.
35. Chen, P. F., Zhu, G. F., Zhang, J. X. (2017). Research on SO_3 removal efficiency by flue gas co-benefit control technique of coal-fired power plants based on field tests. *Environmental Pollution & Control, 39(3),* 232–235. DOI 10.15985/j.cnki.1001-3865.2017.03.002.
36. Li, X. L., Duan, J. X., Li, J. Z., Zhang, W. J. (2017). Control technology and determination methods of SO_3 in flue gas from coal-fired power plants. *Environmental Engineering, 35(5),* 98–102. DOI 10.13205/j.hjgc.201705021.
37. Yi, Y. P., Zhou, D. B., Li, X. L., Zhao, Y. (2017). Research on removal efficiency of low concentration pollutants by wet electrostatic precipitator. *Electric Power Environmental Protection, 33(5),* 26–28. DOI 10.3969/j.issn.1674-8069.2017.05.008.
38. Li, J. W., Fan, L. (2013). Modeling of corona discharge combined with Mn^{2+} catalysis for the removal of SO_2 from simulated flue gas. *Chemosphere, 91(9),* 1374–1379. DOI 10.1016/j.chemosphere.2013.02.028.
39. Yang, Z. D., Chang, Q. Y., Yue, T., Wang, Y., Zheng, C. H. et al. (2015). Experimental study on simultaneous control of SO_2 and PM by wet electrostatic precipitator. *Journal of Engineering Thermophysics, 36(6),* 1365–1370. DOI CNKI:SUN:GCRB.0.2015-06-042.